# Effects on Refrigerant Maldistribution on the Performance of Evaporator

**Jinho Lee†, Chang-Duk Kim*, Ju-Suk Byun, Tae-Sa Jang****

*School of Mechanical Engineering, Yonsei University, Seoul 120-749, Korea*

**Central Region Head Office, Korea Industrial Complex Corp., Gyeong-buk 730-030, Korea*

***Department of Environmental Engineering, Gwangju University, Gwangju 503-703, Korea*

**Key words:** Evaporator, Degree of superheat, Distributor, Circuit arrangement, Tube-by-tube method

**ABSTRACT:** An experimental investigation was made to study two-phase flow distribution in a T-type distributor of slit fin-and-tube heat exchanger using R-22. Experiments were carried out under the conditions of saturation temperature of 5℃ and mass flow rate varying from 0.6 to 1.2 kg/min. The inlet air has dry bulb temperature of 27℃, relative humidity of 50% and air velocity varying from 0.63 to 1.71 m/s. A comparison was made between the predictions from the previously proposed tube-by-tube method and the present experimental data for the heat transfer rate of evaporator. Results show that 82.5% increase of air velocity is needed for T-type distributor with four outlet branches than that of two outlet branches under the superheat of 5℃, which resulted in increasing of air-side pressure drop of 130% for the former as compared to the latter.

## Nomenclature

$C_p$ : specific heat at constant pressure [kJ/(kg·K)]
$h$ : enthalpy [kJ/kg]
$m$ : mass flow rate [kg/s]
$P$ : pressure [Pa]
$Q$ : heat transfer rate [kW]
$RH$ : relative humidity [%]
$T$ : temperature [℃]
$W$ : absolute humidity [$kg/kg_{air}$]
$x$ : quality

### Subscripts

$a$ : air
$cal$ : calculation
$e$ : evaporator
$exp$ : experiment
$fg$ : latent heat capacity
$i$ : inlet
$l$ : latent
$o$ : outlet
$p$ : auxiliary heat exchanger
$r$ : refrigerant
$s$ : sensitive heat
$sat$ : saturate
$sup$ : super heat
$tp$ : two phase
$v$ : vapor
$w$ : water

† Corresponding author
Tel.: +82-2-2123-2816; fax: +82-2-312-2159
*E-mail address*: jinholee@yonsei.ac.kr

## 1. Introduction

Generally, the finned-tube heat exchangers (condensers and evaporators) widely used in

air-conditioning appliances adopt multi-refrigerant circuits to reduce the refrigerant pressure drop. Especially when EEV (Electronic Expansion Valve) whose throttle angle is varied according to the number of electronic pulse is used, the refrigerant enters into each circuit in two-phase ( $x$=0.1 or 0.2) through a distributor. Since distributor configuration, establishment location, air velocity, and temperature profile influence a degree of superheat on the evaporator outlet side and a temperature glide of a fin by conduction, uniform distribution of a refrigerant flow rate is very important for a performance of heat exchangers.[1-2] If the distribution of refrigerant flow rate in each circuit in a multi-circuit evaporator is not equal, the refrigerant at the outlet side of the outdoor coil will go through both single phase and two-phase, inducing an nonuniform profile of air temperature. Consequently, the evaporator with multi-circuit is less efficient because of the widening of superheated vapor region. Therefore if the evaporator with multi-circuit is used, superheated vapor region must reduce as much as possible and uniform distribution of the refrigerant is required at the distributor so that superheated vapor region is evenly distributed.

Kim[3] and Park et al.[4] conducted experimental studies on the distribution of mass flow rate and refrigerant pressure drop in a multi-circuit heat exchanger using R-11 and R-22. Recently, Tae and Cho[1] presented fundamental data for design of a multi-circuit heat exchanger. They investigated the two-phase flow characteristics of refrigerant R-22 in T-type distributor with a horizontal and vertical inlet tube. Domanski[5] developed a program, EVSIM, which incorporates some of the most relevant features of existent models including quasi-local heat transfer analysis of heat exchangers. Youn et al.[6] suggested a model for analyzing cross-flow finned-tube heat exchanger which predicted heat transfer rate of heat exchangers with various circuit configurations within ±4%. Lee et al.[7] developed program that calculates all information related to heat and mass transfer at any local point of heat exchanger to improve the efficiency of zeotropic mixture refrigerant evaporators. The program showed similar trends with experimental results and the deviation between the simulations and test data was a maximum of 5.4%. Beyond these, many analytical attempts have been made for convenient design of a finned-tube heat exchanger increasing the confidence of prediction. For most analytical methods for multi-circuit heat exchangers, mass flow rate of refrigerant flowed in each circuit is assumed uniform just by dividing the total mass flow rate by the number of circuit. However, each mass flow rate of refrigerant at multi-circuit is nonuniform in practice which cast a doubt on the confidence of simulation result. Pressure drop in each circuit is different, because effects of gravity and friction operating in each circuit are different. Pressure difference induces non-uniform mass flow rate of refrigerant.

In this study, it is examined experimently that the effects of maldistribution of refrigerant have on the performance of a multi-circuit finned-tube evaporator. The results are compared with simulation result from the tube-by-tube analysis by Domanski.[5] The tube-by-tube method analyzes heat exchanger by combining results of single tube analysis based on counter flow, mixed refrigerant flow and unmixed air flow for each tube enabling the prediction of performance for the circuit and combining junction.

Experiment is carried out on a heat exchanger with a T-type distributor with R-22 as a working fluid. The number of the circuit adopted is 2, 3 and 4. Air and refrigerant temperature profile, and the degree of superheat of refrigerant at the evaporator outlet are measured by varying the mass flow rate of refrigerant and the number of circuits.

## 2. Experiment

### 2.1 Experimental apparatus

The schematic diagram of the experimental apparatus is shown in Fig. 1. The system mainly consists of an air loop, a refrigerant loop, and a test heat exchanger. The air loop is a close-circuit wind tunnel. Its airflow is driven by a 3.7 kW axial fan to be controlled with an inverter. To avoid or minimize the effect of non-uniform flow distribution, a honeycomb and 4 screens are provided. The temperature and humidity of the air-stream are controlled in a flow conditioning chamber. The magnetic gear pump instead of a compressor circulates the refrigerant to eliminate the effect of the refrigeration oil. The magnetic gear pump is driven by a variable speed DC motor. The refrigerant used in this test, R-22, must achieve the subcooled liquid state before entering the magnetic gear pump. A brazed plate heat exchanger is used as an additional cooler to prevent incomplete condensation of the refrigerant before passing through a test heat exchanger. Both the pressure and the temperature regulating tank constantly maintain the pressure and temperature of the refrigerant which enters into the heat exchanger. The degree of superheat of the refrigerant is controlled by the counter flow type double-pipe heat exchanger using water as heat transfer medium. Refrigerant temperature is measured by T-type thermocouples at the test heat exchanger inlet and outlet. Pressures are measured by the pressure transducers with an accuracy of ±2% placed near thermocouples. The mass flow meter is installed in liquid line to measure the refrigerant mass flow rate. Its accuracy is ±1%.

The test heat exchanger is the cross counter-flow type with 3 row circular copper tubes and aluminum slit fins. Its overall dimensions are 400×400×80 mm (width×hight×depth). The finned-tube heat exchanger is installed such that tube is horizontal and fins is vertical. The outside diameter of the tube is 9.52 mm. Also a micro-fin is machined inside the tube. The circuit arrangement of a test heat exchanger is lower portion type in which the location of the refrigerant inlet position is lower and the location of the refrigerant outlet position is upper.

Refrigeration and air flow directions and the configurations of distributor for each circuit is shown Figs. 2 and 3. As shown in Fig. 3, the angles of branch tube at each circuit are 180° (2-circuit), 120° (3-circuit), 90° (4-circuit), re-

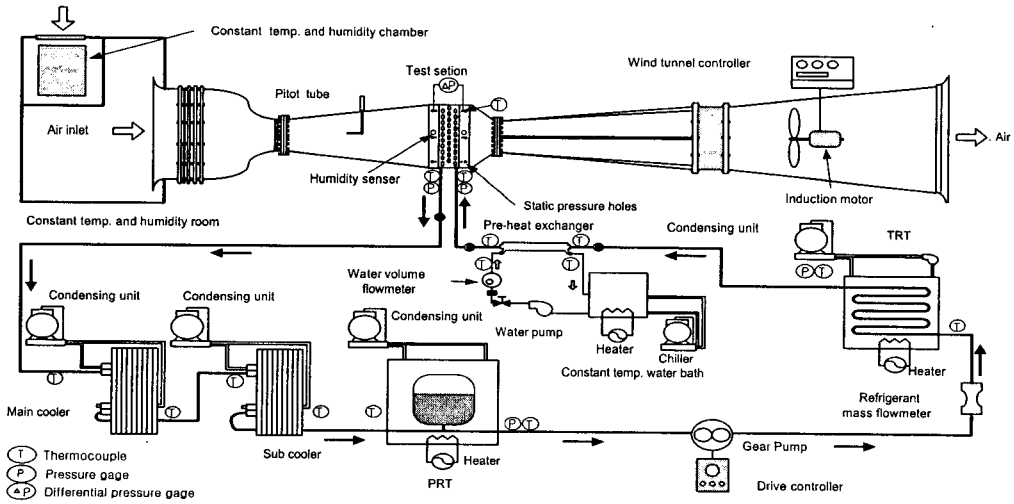


Fig. 1 Schematic diagram of experimental apparatus for evaporator test system.

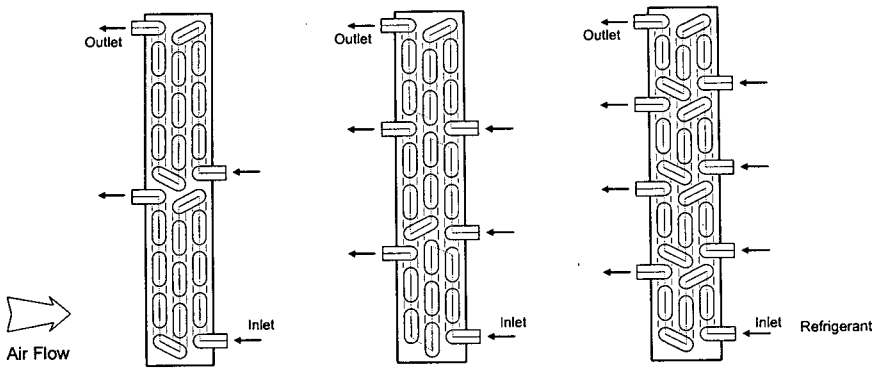


(a) 2-circuit (b) 3-circuit (c) 4-circuit

Fig. 2 Flow diagram of refrigerant and air.

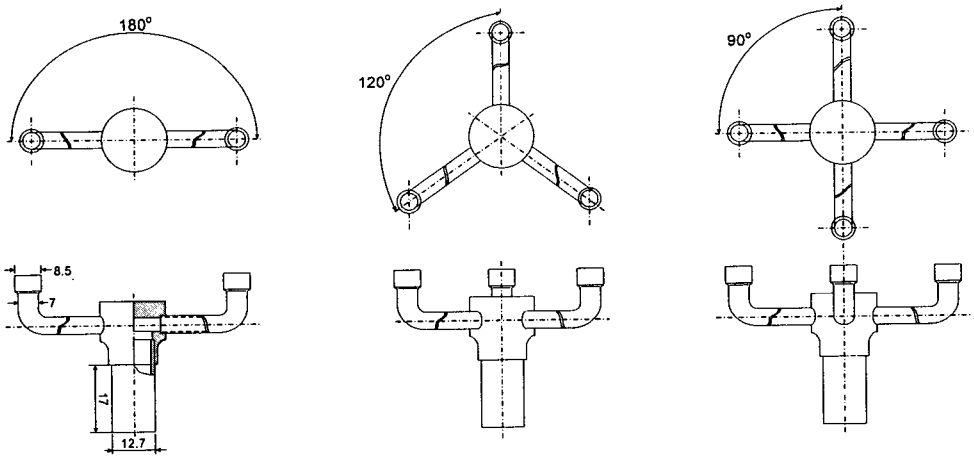


(a) Distributor for 2-circuit (b) Distributor for 3-circuit (c) Distributor for 4-circuit

Fig. 3 Schematic drawing of refrigerant distributor configurations (all dimensions in mm).

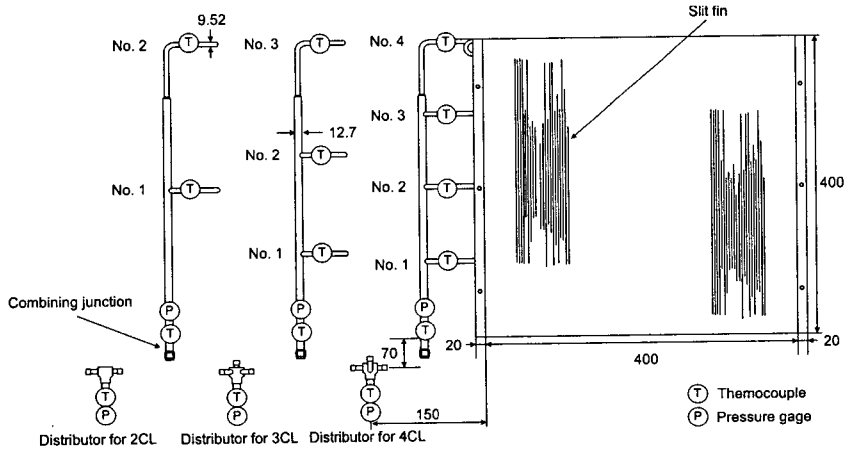


Fig. 4 Schematic drawing of combining junctions and slit fin-and-tube heat exchanger configurations (all dimensions in mm).

spectively. To measure the pressure and temperature of refrigerant in the evaporator exit, T-type thermocouples and pressure transducers are installed at each circuit exit and combining junction as shown in Fig. 4.

### 2.2 Experimental conditions and method

Refrigerant flow rate distribution for each circuit isn't uniform due to the effects of friction and gravity. This study analyzes effects of refrigerant maldistribution by exit air temperature of each circuit instead of mass flow rate of refrigerant. Table 1 shows experimental conditions and Table 2 specifies measuring devices, respectively. Air velocity and pressure drop are measured to estimate the required values in maintaining the degree of superheat of 5℃ at combining junction of circuit at the evaporator exit, while keeping the mass flow rate of re-

Table 1 Experimental conditions

| | | |
|---|---|---|
| Air-side | Dry bulb temperature of air at the evaporator inlet | 27℃ |
| | Standard relative humidity at the evaporator inlet | 50% |
| | Face velocity at the evaporator inlet | 0.63~1.71 m/s |
| Refrigerant-side | Refrigerant | R22 |
| | Quality at the evaporator inlet | 0.1 |
| | Refrigerant mass flow rate | 0.6, 0.8, 1.0, 1.2 kg/min |
| | Evaporation temperature | 5℃ |
| | Degree of superheat | 5℃ |

Table 2 Specification of measuring device

| | Manufacturer | Model | Range | Error (Full scale) |
|---|---|---|---|---|
| T-type thermocouple | Omega | FF-T-30 | −60~200℃ | ±0.1℃ |
| Micro manometer | Furness controls Inc. | FCO12 | 0~19.99 mm$H_2O$ | ±1%/1.95 Pa |
| Mass flow meter | Oval | D025S-SS-200 | 0~10 kg/min | ±0.2% |
| Volume flow meter | Kytora | Gear meter 2950 | 0.04~4.0 L/min | ±1% |
| Pressure transmitter | Setra | C230 | 0~3447 kPa | ±0.25% |
| Thermocouple reference unit | ISOTECH | 1310 | 0℃ | ±0.01% |
| Humidity transmitter | Sam won Eng. | $d_i$ : 10 mm<br>L : 250 mm | 0~100% | ±3% |

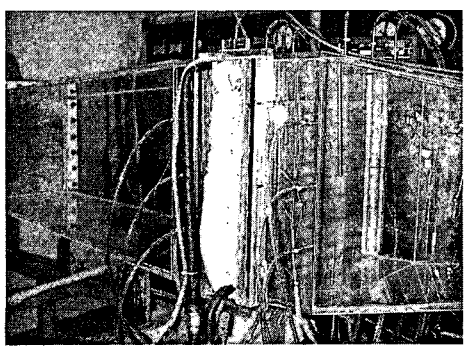

(a) Test section

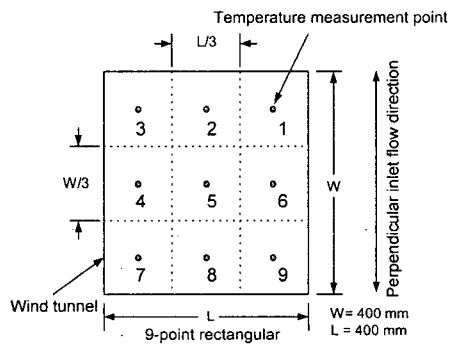


(b) Measurement location

Fig. 5 Measurement location (b) for air temperature at inside test section (a).

frigerant constant. As shown in Fig. 5, the air temperature at the exit of the test section is measured with nine T-type thermocouples which are installed 10 mm behind the evaporator, each located at the center of equally divided nine flow area of whole flow cross section. The airside pressure drop which occurs at the main test section is measured with 24 static pressure taps, each half of them is placed on the front and rear acryl wall of the evaporator, respectively. Refrigerant temperatures at each circuit and combining junction are measured by a T-type thermocouple inserted in the tube. The measurement starts when the air and the refrigerant inlet state come to be within ±3℃ of temperature and ±2% of pressure. Data from each sensor are recorded at 3 seconds intervals for 5~10 minutes by the data acquisition equipment. Moist air properties are calculated based on ASHRAE Fundamentals Handbook,[8] and the properties of R-22 are based on REFPROP Ver 6.01.[9]

## 3. Simulation

The simulation was performed based on the tube-by-tube analysis suggested by Domanski, using a complete set of correlations for the heat transfer and pressure drop in the evaporator (Table 3). The tube-by-tube analysis repeatedly calculates data of each tube to find exit state from inlet state of finned-tube heat exchanger, and inlet air temperature of second row is obtained from the arithmetic mean temperature of adjacent two tube of the front row. The prediction is made for the performance of the finned-tube heat exchanger (evaporator) by evaluating individual tube in this way. The program used for the simulation consists of three subprograms. The first program calculates the property of air and refrigerant according to temperature and pressure of each tube. The second program calculates the heat transfer coefficient and pressure drop from results of the first program. The final third program calculates degree of the superheat and saturated pressure of refrigerant in the combining junction of evaporator exit.

The evaporator simulation program using the tube-by-tube analysis should insert the shape function of a heat exchanger, degree of superheat, and operation conditions, together with the assumptions for the saturated temperature and mass flow rate of R-22. The degree of superheat and saturated pressure obtained from the simulation program are compared with the

Table 3 Correlations used for the simulation of evaporator

| Items | | Applying zone | Correlations | Remark |
|---|---|---|---|---|
| Refrigerant-side heat transfer coefficient | | Two-phase<br>Single-phase | Gungor and Winterton[10]<br>Wang et al.[11] | Smooth tube<br>Micro-fin tube |
| Heat transfer enhancement factor | | | Schlager et al.[12] | |
| Refrigerant-side pressure drop | Straight tube | Two phase<br>Single phase | Haraguchi et al.[13]<br>Carnavos[14] | Micro-fin tube |
| | Bend tube | Two phase<br>Single phase | Geary[15]<br>Ito[16] | Smooth tube |
| Penalty factor for micro-fin tube | | | Schlager et al.[17] | |
| Air-side heat transfer coefficient | | | Wang et al.[18] | Slit fin |
| Fin efficiency<br>Contact conductance<br>Air property<br>Refrigerant property | | | McQuiston and Parker[19]<br>Natio[20]<br>ASHRAE handbook[8]<br>REFPROP 6.01[9] | |

previous pressure condition. If the difference is within $10^{-5}$, the calculation is ended, or the computations are repeated until convergence is obtained. The calculation of pressure drop at the refrigerant-side takes into account the effect of gravity and friction between the straight tube section and U-bend tube section. The simulation results were compared with experimental results.

## 4. Data reduction

### 4.1 Quality of refrigerant

The refrigerant quality at the inlet of the evaporator is calculated from transferring heat from the hot water of an auxiliary heat exchanger to R-22.

$$Q_p = m_w C_{p,w}(T_{w,p,i} - T_{w,p,o}) \quad (1)$$

$$Q_p = Q_{p,s} + Q_{p,l} \quad (2)$$

$$Q_{p,s} = m_r C_{p,r}(T_{r,p,o} - T_{r,p,i}) \quad (3)$$

$$Q_{p,l} = m_r h_{fg,r} x_{p,o} \quad (4)$$

$$x_i = x_{p,o} = \frac{1}{h_{fg,r}}\left[\frac{Q_p}{m_r} - C_{p,r}(T_{r,p,o} - T_{r,p,i})\right] \quad (5)$$

where, $Q$, $C_p$, $m$, $T$, $h$, $x$ mean heat transfer rate, specific heat, mass flow rate, temperature, enthalpy, and refrigerant quality respectively. Subscripts, $p$, $w$, $i$, $o$, $s$, $l$, $fg$ represent an auxiliary heat exchanger, water, inlet, outlet, sensible heat, latent heat and latent heat capacity, respectively.

### 4.2 Heat transfer rate

If the fin surface temperature of an evaporator is lower than dew point, condensation occurs on the fin surface. Therefore, a heat transfer rate of the airside is obtained by summing sensible heat capacity and latent heat capacity.

$$Q_a = Q_{a,s} + Q_{a,l} \quad (6)$$

$$Q_{a,s} = m_a C_{p,a}(T_{a,i} - T_{a,o}) \quad (7)$$

$$Q_{a,l} = m_a(W_{a,i} - W_{a,o}) h_{fg,w} \quad (8)$$

$$Q_r = Q_{tp} + Q_v \quad (9)$$

$$Q_{tp} = m_r(1 - x_i)(h_{v,r} - h_{l,r}) \quad (10)$$

$$Q_v = m_r(h_{s,r} - h_{v,r}) \quad (11)$$

The heat transfer rate of the evaporator is calculated by the arithmetic mean of the heat transfer rate of both the air and refrigerant as in Eq. (12) and the difference between them remained within ±8%.

$$Q_e = \frac{Q_r + Q_a}{2} \quad (12)$$

## 5. Results and discussion

### 5.1 Air temperature profile

Figure 6 represents the air temperature profile at the evaporator outlet according to the refrigerant mass flow rate and the number of circuit when evaporate temperature is maintained at 5℃ and the degree of superheat at the evaporator outlet is maintained at 5℃. The test range for mass flow rate of refrigerant is 0.6~1.2 kg/min.

Experimental result for 2-circuit is shown in Fig. 6(a). Each circuit has 24 tubes and angle of branch tubes is 180°. Average air temperature in the evaporator exit is 7.1℃ which is close to 5℃, the evaporate temperature of refrigerant. For the overall test range of the mass flow rate of refrigerant, the temperature of the upper part of evaporator (No. 1-3 of Fig. 5(b)) is 9~14% higher than those of lower part (No. 7-9 of Fig. 5(b)). This is because the lower part temperature represent the temperature of refrigerant in evaporate process, while the upper part temperature is influenced by the temperature of refrigerant near exit stage of

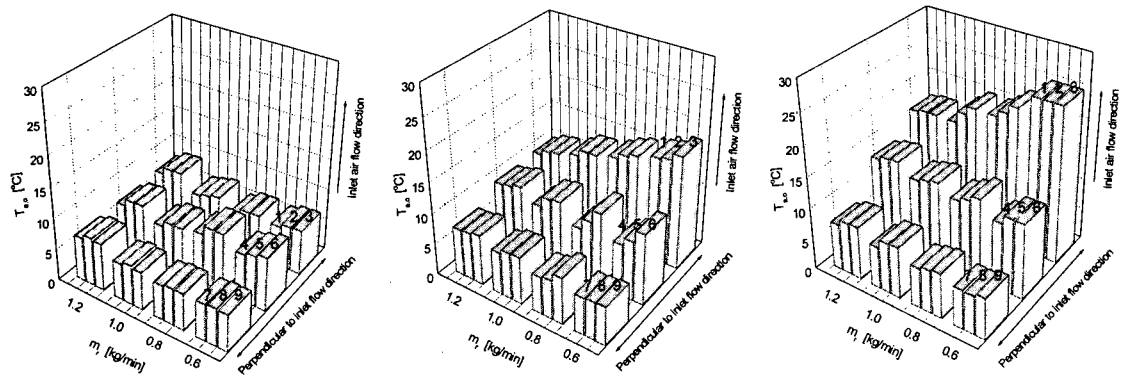


(a) 2-circuit (b) 3-circuit (c) 4-circuit

Fig. 6 Air temperature profile at the evaporator outlet according to the refrigerant mass flow rate and the number of circuit.

refrigerant circuit which is at a higher temperature than the refrigerant near inlet and mid region.

Figure 6(b) represents results for 3-circuit. For the 3-circuit, each circuit has 16 tubes and the angle of branch tubes is 120°. The air temperature profile in this case at the evaporator exit is more uninformed than that of 2-circuit. When mass flow rate of refrigerant is 0.6 kg/min, the air temperature of the lower part of the evaporator is 6℃, and that of the upper part is 17.3℃. This is because the circuit located on the upper end is more influenced by pressure drop due to the friction and gravity than the circuit located on the lower end. At the evaporate temperature of 5℃, vapor density of the R-22 is 24.79 kg/m$^3$ and its liquid density is 1,264 kg/m$^3$, which is 50 times that of vapor density. Therefore, the flow rate of the refrigerant of the vapor state increases as a circuit is located in the upper end due to the increased vapor quantity. This also induces reduction of latent heat capacity, a rise in the degree of superheat at the upper circuit exit, and a drop of cooling performance of the evaporator at the upper circuit. When mass flow rate of refrigerant increases to 1.2 kg/min, the average air temperature difference between upper and lower of the evaporator is about 3℃, much less than that of 0.6 kg/min.

Figure 6(c) represents results for 4-circuit. For this case, each circuit has 12 tubes and the angle of branch tubes is 90°. When mass flow rate of refrigerant is 0.6 kg/min, air temperature of the evaporator at upper part is 25.2 ℃, which is close to 27℃, the air temperature of the evaporator inlet. That of the lower part is 6.3℃ which is similar to the temperature profiles of the (a) and (b). For the 4-circuit evaporator, it is hard to maintain the degree of superheat at the combining junction at 5℃ because the degree of superheat largely differs in each circuit exit, and throttle angle variation of EEV is unstable.

These test results show that increasing mass flow rate of the refrigerant makes the outlet air temperature profile of the evaporator more uniform and at the same time increasing the number of circuits causes the non-uniformity of the outlet temperature.

### 5.2 Air velocity and pressure drop of airside

Figure 7 presents required air velocity to maintain the degree of superheat at 5℃ at each evaporator for 2-circuit, 3-circuit, 4-circuit, respectively. Test results show that the required air flow rate to maintain the degree of

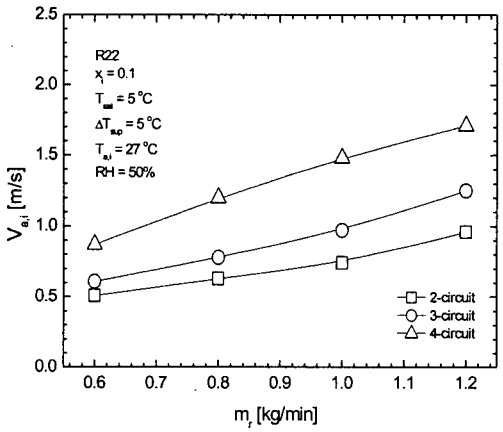


Fig. 7 Required air velocity to maintain the degree of superheat at 5℃ at each evaporator.

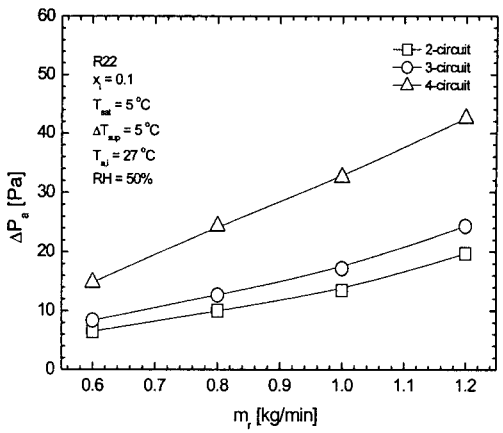


Fig. 8 Airside pressure drop for the air velocity.

superheat at 5℃ increases as the number of circuits and the mass flow rate of refrigerant increase. Air velocities for 3-circuit and 4-circuit should be increased 27% and 85.2%, respectively more than that of the 2-circuit to maintain the 5℃ superheat condition. If the number of circuits increases, the distribution of refrigerant between circuits becomes more non-uniform due to the refrigerant pressure drop. The mass flow rate of refrigerant in the upper circuit becomes smaller and that in the lower circuit becomes lager, thus in the upper circuit, refrigerant evaporates faster and the refrigerant temperature of the circuit outlet increases. On the other hand, the lower circuit needs the higher air flow rate to evaporate refrigerant and to maintain the degree of superheat due to the larger mass flow rate of refrigerant. This indicates that if the number of circuit increases, and fan speed is constant, energy consumption for maintaining the performance of the system increases.

Figure 8 shows the airside pressure drop for the air velocity given in Fig. 7. For all the mass flow rate of refrigerant, the airside pressure drop of 3-circuit and 4-circuit is 26% and 130 % larger than that of the 2-circuit, respectively. Therefore, maldistribution of refrigerant between the circuits affects the fan power which is influenced by both air velocity and airside pressure drop.

### 5.3 Comparison of experiment and simulation

Figure 9 compares the experiment results on refrigerant temperature of each circuit outlet with simulation results by the tube-by-tube analysis. The more the number of circuit is, the larger the difference of results between ex-

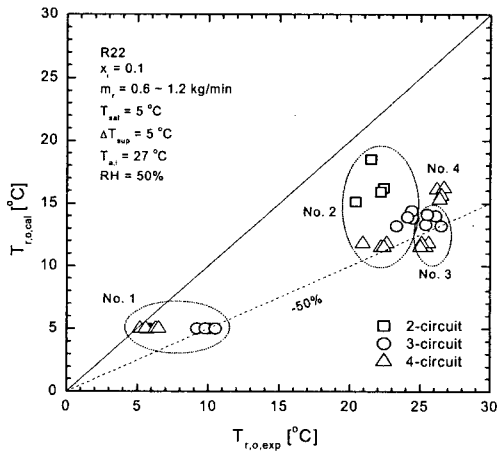


Fig. 9 Comparison of experiment and simulation results for refrigerant temperature at each circuit outlet.

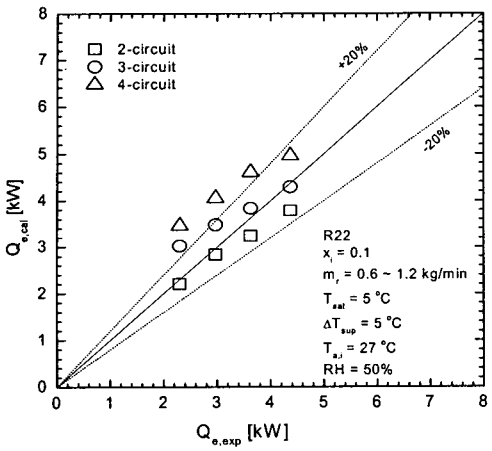


Fig. 10 Comparison of experiment and simulation results for heat transfer rate at each circuit outlet.

periment and simulation. There was 35% difference between results for the outlet refrigerant temperature of the upper circuit in the case of a 2-circuit heat exchanger. But, for that of the lower circuit, the difference was only 2%. For a 3-circuit heat exchanger, outlet temperature of the second circuit from the test is 55% smaller than that of the simulation. For the third circuit of a 4-circuit heat exchanger, the difference was 68%. In Fig. 10, the heat transfer rate obtained from experiment was compared with that from the simulation. Generally, the average deviations between experiment and simulation results increases as the circuit number increases, but they differs depending on the refrigerant mass flow rate and the number of circuit. When mass flow rate of refrigerant is 0.6 kg/min, the differences between the experiment and simulation results in the case of 2-circuit, 4-circuit were 0.4%, 31.6% respectively. When mass flow rate of refrigerant is 1.2 kg/min, the trend is reversed and the differences for 2-circuit, and 4-circuit were 50.5%, 13.5%, respectively. Thus, the more mass flow rate of refrigerant is, the larger the difference between experiment and simulation results at the 2-circuit evaporator, while the smaller the difference between experimental results at the case of 4-circuit evaporator. From the above discrepancy between experimental and simulation results for multi-circuit heat exchanger, it is required that the refrigerant distributor for the evaporator be chosen to distribute refrigerant between circuits as to satisfy the refrigerating load at each circuit. Also in the simulation, the refrigerant distribution characteristics in each circuit should be considered for the accurate prediction of evaporator performance with high reliability.

## 6. Conclusion

Experiment is carried out with R-22 to see the effect of maldistribution of refrigerant on the performance of the evaporator. Three types of evaporators were used in this test; 2-circuit, 3-circuit, 4-circuit and distributor was T-type. The results are compared with simulation results, and can be summarized as follow.

(1) The maldistribution of refrigerant between the circuits increased with less mass flow rate of refrigerant and with the number of circuit. The maldistribution of refrigerant caused the instability of degree of the superheat at the combining junction of the evaporator.

(2) Air velocity of 3-circuit and 4-circuit required to maintain the degree of superheat at 5℃ was 27%, 85.2% higher than that of the 2-circuit, respectively. At this air velocity, the airside pressure drop of 3-circuit and 4-circuit was 26%, 130% larger than that of the 2-circuit, respectively. Maldistribution due to the increase of the number of circuits brought the increase of fan power consumption, indicating lower performance.

(3) The average deviations between experiment and simulation results increases as the circuit number increases, but they differs depending on the refrigerant mass flow rate and the number of circuits.

(4) It is required that the refrigerant distri-

butor for the evaporator be chosen to distribute refrigerant between circuits as to satisfy the refrigerating load at each circuit.

## Appendix A

The uncertainty analysis for experiment is performed by the method which is suggested by Kline and McClintock.[21] The calculation divides by air side and refrigerant side. The heat transfer rate for airside is calculated using the measured temperature and flow rate of air. The uncertainty for that is represented as following

$$\frac{\delta Q_a}{Q_a}=\sqrt{\left(\frac{\delta m_a}{m_a}\right)^2+\left(\frac{\delta C_p}{C_p}\right)^2+\left(\frac{\delta T_{a,i}}{T_{a,i}}\right)^2+\left(\frac{\delta T_{a,o}}{T_{a,o}}\right)^2} \quad \text{(A1)}$$

where specific heat, $C_p$, is obtained by temperature and pressure. The mass flow rate of air, $m_a$, is estimated by multiplying the density, cross sectional area and air velocity, and uncertainty for that can be represented as follows,

$$\frac{\delta m_a}{m_a}=\sqrt{\left(\frac{\delta \rho_a}{\rho_a}\right)^2+\left(\frac{\delta A_a}{A_a}\right)^2+\left(\frac{\delta V_a}{V_a}\right)^2} \quad \text{(A2)}$$

The measurement uncertainty level of thermocouple and micro manometer are ±0.1℃, ±1% for 1.95 Pa after calibrating the thermocouples and the micro manometer and the date acquisition system, as shown Table 2. The uncertainty for mass flow rate of air is 4%, and the uncertainty of specific heat and temperature are 0.98% and 0.4%, respectively. Therefore overall uncertainty of heat transfer rate for air is 4.2%.

The heat transfer rate of the refrigerant side was estimated by multiplying the mass flow rate and the enthalpy difference. The heat transfer rate for the refrigerant side was lead to Eq. (A3).

$$\frac{\delta Q_r}{Q_r}=\sqrt{\left(\frac{\delta m_r}{m_r}\right)^2+\left(\frac{\delta h_{r,i}}{h_{r,i}}\right)^2+\left(\frac{\delta h_{r,o}}{h_{r,o}}\right)^2} \quad \text{(A3)}$$

where mr is the refrigerant mass flow rate. The mass flow meter has a measurement error of ±0.2%. Since the enthalpy of the refrigerant is calculated using the measured temperature and pressure, the source of uncertainty for the enthalpy difference is related to the error of the temperature and pressure measurements at the inlet and outlet of the evaporator. The uncertainty of the enthalpy is estimated 0.5%. Therefore, the uncertainty for the heat transfer rate of the refrigerant side is 0.7%.

## References

1. Tae, S. J. and Cho, K., 2002, Two-phase flow characteristics of refrigerant in T-branch with horizontal and vertical inlet tube, Korean Journal of Air-Conditioning and Refrigeration Engineering, Vol. 14, No. 9, pp. 741-748.
2. Kim, C. D., Jeon, C. D. and Lee, J., 2003, Effects of the temperature glide and superheat of R407C on the performance of evaporator, Korean Journal of Air-Conditioning and Refrigeration Engineering, Vol. 15, No. 10, pp. 852-859.
3. Kim, J. S., 1993, Two phase flow distribution in multi-parallel evaporator tubes (1st report: Non-heating mode), Refrigeration-Air Conditioning Engineering, Vol. 12, No. 1, pp. 1-20.
4. Park, J. H., Cho, K. and Cho, H. G., 1999, Characteristics two-phase flow distribution and pressure drop in a horizontal T-type evaporator tube, Korean Journal of Air-Conditioning and Refrigeration Engineering, Vol. 11, No. 5, pp. 658-668.
5. Domanski, P. A., 1989, EVSIM-An Evaporator Simulation Model Accounting for Refrigerant and One Dimensional Air Distribution, NISTIR 89-4133.

6. Youn, B., Park, H. Y. and Kim, C. H., 1998, Analytical model of dry surface cross-flow fin-tube heat exchanger by tube-by-tube method, Proceedings of the SAREK '98 Summer Annual Conference, pp. 1399-1404.
7. Lee, J. H., Kwon Y. C. and Kim M. H., 2003, An improved method for analyzing a fin and tube evaporator containing a zeotropic mixture refrigerant with air mai-distribution, International Journal of Refrigeration, Vol. 26, pp. 707-720.
8. ASHRAE, 1993, Fundamental Handbook (SI).
9. McLinden, M. O., Klein, S. A., Lemmon, E. W. and Peskin, A. P., 1998, Thermodynamic and transport properties of refrigerants and refrigerant mixtures database (REFPROP), Ver. 6.01, NIST.
10. Gungor, K. E. and Winterton, R. H. S., 1986, A general correlation for flow boiling in tubes and annuli, International Journal of Heat and Mass Transfer, Vol. 19, No. 3, pp. 351-358.
11. Wang, C. C., Chiou, C. C. and Lu, D. C., 1996, Single-phase heat transfer and flow friction correlation for micro fin tubes, International Journal of Heat and Fluid Flow, Vol. 17, pp. 500-508.
12. Schlager, L. M., Pate, M. B. and Bergles, A. E., 1990, Performance predictions of refrigerant oil mixtures in smooth and internally finned tube, II, design equations, ASHRAE Transaction, Vol. 96, pp. 170-182.
13. Haraguchi, H., Koyama, S., Esaki, J. and Fujii, T., 1993, Condensation heat transfer of refrigerants HFC134a, HCFC123 and HCFC22 in horizontal smooth tube and a horizontal microfin tube, Proc., 30th National Symposia of Japan, Yokohama, pp. 343-345.
14. Carnavos, T. C., 1980, Heat transfer performance of internally finned tube, Heat Transfer Engineering, Vol. 4, p. 32.
15. Geary, F. D., 1975, Return bend pressure drop in refrigeration system, ASHRAE Transactions, No. 2342, pp. 252-265.
16. Ito, H,. 1960, Pressure loses in smooth pipe bends, Basic Engineering, Transaction of ASME, Vol. 3, p. 135.
17. Schlager, L. M., Pate, M. B. and Bergles, A. E., 1989, Heat transfer and pressure drop during evaporation and condensation of R-22 in horizontal micro-fin tubes, International Journal of Refrigeration, Vol. 12, pp. 6-14.
18. Wang, C. C., Tao, W. H. and Chang, C. J., 1999, An investigation of the airside performance of the slit fin-and-tube heat exchangers, International Journal of Refrigeration, Vol. 22, pp. 595-603.
19. McQuiston, F. C. and Parker, J. D., 1994, Heating, Ventilating, and Air Conditioning Analysis and Design, John Wiley & Sons, pp. 543-547.
20. Natio, N., 1970, SHASE Transactions (The Society of Heating, Air-conditioning and Sanitary Engineers of Japan), Vol. 44, pp. 1-5.
21. Kline, S. J. and McClintock, F. A., 1953, Describing uncertainty in single sample experiments, Mechanical Engineering, Vol. 75, pp. 3-8.